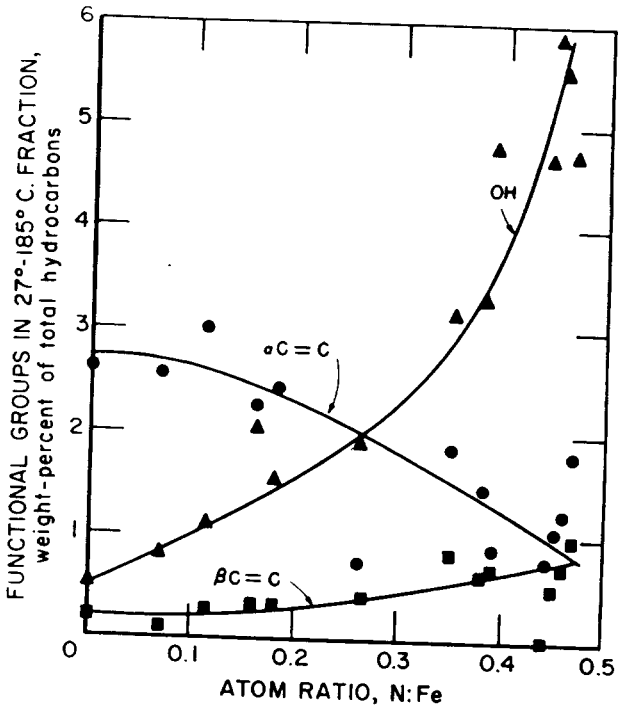

FIGURE 24.—Effect of Initial Nitrogen Content of Catalyst on Alcohol and Olefin Production.

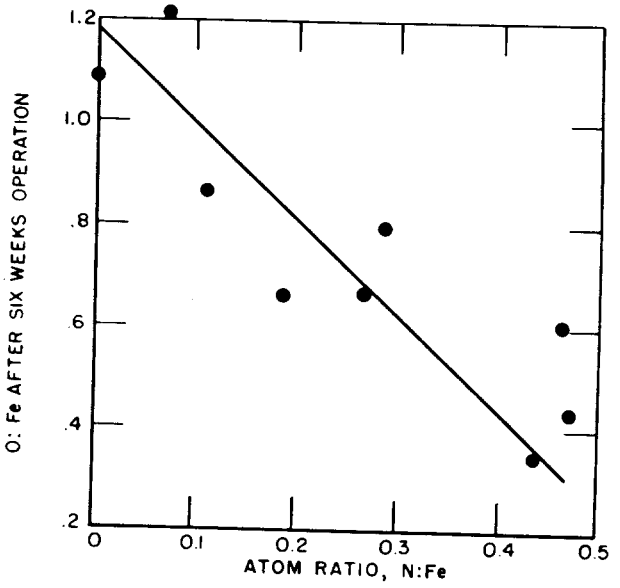

FIGURE 25.—Effect of Initial Nitrogen Content on Oxidation of Catalyst During Synthesis.

was generally the principal phase. In previous experiments (*42*) at atmospheric pressure with synthesis gas or carbon monoxide, a sample with N:Fe=0.08 was converted to Hägg carbide, another with N:Fe=0.21 to ϵ-carbonitride, and a third with N:Fe=0.29 to ϵ-carbonitride. During synthesis, the carbon and oxygen contents of the partly nitrided samples increased more rapidly than for fully nitrided ϵ-iron nitrides under the same conditions.

Thus, the experiments on partly nitrided catalysts show that the ϵ-iron carbonitride does not form in the synthesis unless nitriding has already established the ϵ-iron nitride phase. Other forms of nitrides revert to metallic iron, iron carbides, magnetite, and perhaps other phases that are more readily oxidized and are characteristic of the operation of reduced or carbided iron catalyst.

SYNTHESIS TESTS WITH IRON CATALYSTS CONVERTED TO ϵ-IRON CARBONITRIDE

A series of ϵ-iron carbonitrides prepared prior to synthesis was also tested (*70*). All experiments were made with 6- to 8-mesh particles of fused catalyst D3001. Pretreated and used catalysts were analyzed by chemical methods for iron, carbon, and nitrogen, and oxygen was determined by difference. Phases present were identified by X-ray diffraction. The nature and sequence of pretreatment steps, chemical composition, and phases in pretreated and used catalysts are given in table 17. The symbols, C:Fe, N:Fe, and O:Fe denote the atomic ratios of carbon, nitrogen, and oxygen to iron.

To study the effect of preparational variables (table 17), carbonitrides were prepared by nitriding reduced catalysts in ammonia and then carbiding with carbon monoxide (X287, X252, and X279), by carbiding with carbon monoxide and then nitriding with ammonia (X407), or by simultaneous carbiding and nitriding with methylamine (X739). For comparison, carbided catalysts containing no nitrogen are included (X342 and X294).

In the ensuing synthesis tests, the ϵ-iron carbonitride persisted throughout the experiments. The catalyst of test X739 was not completely reduced before treatment with methylamine; however, based on the part of the catalyst that was reduced, N:Fe and C:Fe ratios were, respectively, 0.08 and 0.24. As only the outer layer of the catalyst is effective in the synthesis, this test is probably comparable, despite the lower extent of reduction.

In figures 26 and 27, the activities and selectivities of the carbonitrided catalysts of table 17 are shown for experiments conducted at 7.8 and 21.4 atmospheres operating pressure. As in previous presentations of selectivity, only hydrocarbons and oxygenated molecules dissolved in liquid hydrocarbons are considered. Data for carbided (tests X294 and X342) and nitrided catalysts (tests X215 and X225) are

TABLE 17.—*Pretreatment, composition, and activity of carbonitrides formed before synthesis*

(All pretreatments at atmospheric pressure. All synthesis tests at 21.4 atmospheres except where noted)

Test X—	Reduction in hydrogen [1]			Second pretreatment [2]			Third pretreatment [2]			Composition of pretreated catalysts				Catalyst composition after synthesis				Activity [3] per gram Fe A_{Fe}
	Temperature, ° C.	Time, hour	Reduction, percent	Reagent	Temperature, ° C.	Time, hour	Reagent	Temperature, ° C.	Time, hour	C:Fe	N:Fe	O:Fe	Component phases [4]	C:Fe	N:Fe	O:Fe	Component phases	
342	500	24	97.2	CO	150–350	18				0.57	0	0.07	χ, α	0.49	0	1.48	M, α, S	95
294 [5]	500	24	96.6	CO	150–350	18				.58	.0	.03	χ, α	.71	.0	.37	χ, M	52
287	550	20	97.9	NH_3	350	6	CO	450	10	.62	.02	.16	χ, M	.63	.02	.32	χ, M	65
252 [5]	550	20	96.4	NH_3	400	1	CO	350	6	.19	.29	.03	ϵ				ϵ	69
279	550	20	97.8	NH_3	400	1	CO	350	6	.30	.23	.08	ϵ	.42	.15	.60	ϵ, M, χ	108
407	550	22	96.0	CO	150–250	12	NH_3	350	28	.21	.29	.13	ϵ	.44	.08	.81	ϵ, M	93
739	450	24	63.4	CH_3NH_2	250	16				.15	.05	.85	M, ϵ	.24	.02	1.09	M, ϵ	114

[1] Space velocity of 2,300 to 2,700 hr.$^{-1}$ in all tests.
[2] Space velocity of NH_3: 950 to 1,050 hr.$^{-1}$. Space velocity of CO: 95 to 105 hr.$^{-1}$. Space velocity of methylamine: 1,000 hr.$^{-1}$
[3] Activity defined in chapter on synthesis tests with carbides of iron.
[4] α=metallic iron; χ=Hägg carbide; M=magnetite; S=$MgCO_3$ or $FeCO_3$; ϵ=ϵ-nitride or ϵ-carbonitride.
[5] Tested at 7.8 atmospheres.

included for comparison. Increased production of alcohols and decreased production of high-boiling products were characteristic of the catalysts containing nitrogen, with the exception of test X287, wherein nitriding was insufficient to produce the ϵ phase when subsequently carbided with carbon monoxide. As a result, only χ phase was formed, and therefore this catalyst behaved more like the carbide in test X294.

Activity values for ϵ-nitrides and ϵ-carbonitrides prepared by carburizing nitrides were usually greater than for reduced or carbided catalysts, or for ϵ-carbonitrides prepared from carbide.

Both nitrided and reduced catalysts were oxidized more rapidly at 21.4 than at 7.8 atmospheres, but the nitrides absorbed oxygen at lower rates at both pressures. Carburized catalysts oxidized more rapidly at the higher pressures (*16*, *71*). The depletion in nitrogen was not noticeably affected by pressure. Specifically, this means that the percentage of iron present as ϵ-carbonitride decreases more rapidly at the higher pressure, and the carbon to nitrogen ratio in the ϵ-iron carbonitride increases more slowly at the higher pressure. Therefore, nitrogen is replaced by carbon more slowly, relative to the oxidation reaction at the higher pressure, or carbonitrides rich in carbon are more rapidly oxidized than those that are carbon poor.

ϵ-Carbonitrides prepared by treating nitrides with carbon monoxide had about the same activity as carbonitrides produced during synthesis, shown in all the experiments here reported. ϵ-Carbonitride prepared by nitriding χ-iron carbide with ammonia showed lower activity and formed products with a slighly higher molecular weight than carbonitrides produced in the reverse order. More extensive carburization of a nitride to remove the nitrogen fairly completely produced χ-iron carbide that had the same catalytic properties as the χ-iron carbide produced by direct carburization of a reduced catalyst. The ϵ-carbonitride from methylamine produced the low molecular weight product characteristic of ϵ-carbonitrides; however, a smaller amount of oxygenated compounds and more olefins were formed.

In other studies reduced catalyst D3001 was treated with methylamine in a glass apparatus; however, the principal phase was Hägg carbide in all of these experiments. Figure 28 presents plots of the atomic ratios of carbon and nitrogen to iron as a function of time for experiments at 200° and 250° C. At 250° C. the reaction appeared to be essentially complete after 7 hours, and the atomic concentration of carbon was about 3 times that of nitrogen. At 200° C. the ratio of nitrogen to carbon introduced into the catalyst was about 6 to 10 on an atomic basis, but the reaction was slow at this temperature. At 300° C. the deposition of carbon was more rapid, and the ratio of ntrogen to carbon was appreciably less than at 250° C.

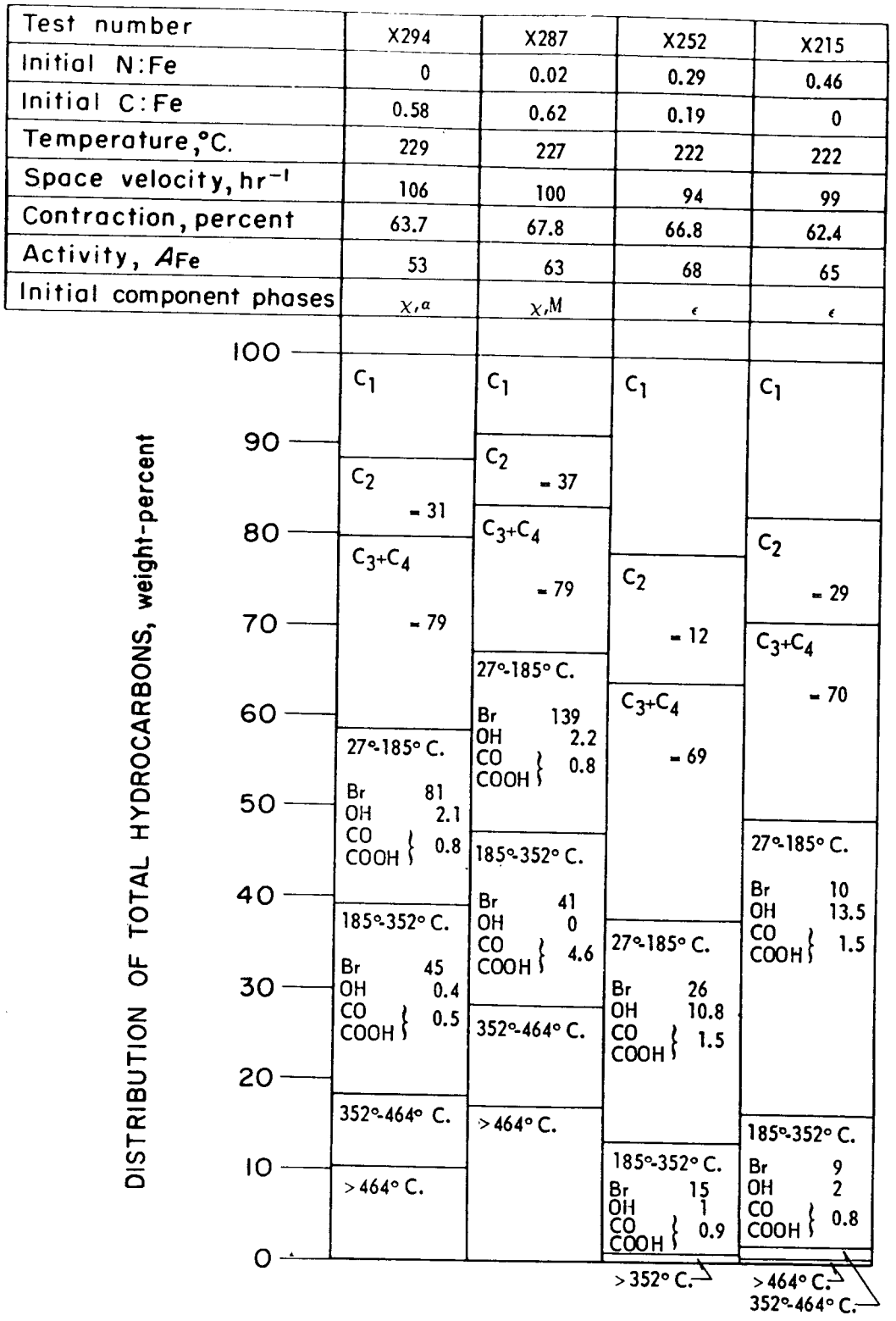

FIGURE 26.—Activity and Product Distribution From Carbonitrided Catalysts With $1H_2+1CO$ Gas at 7.8 Atmospheres. Total hydrocarbons includes oxygenated material dissolved in liquid phase.

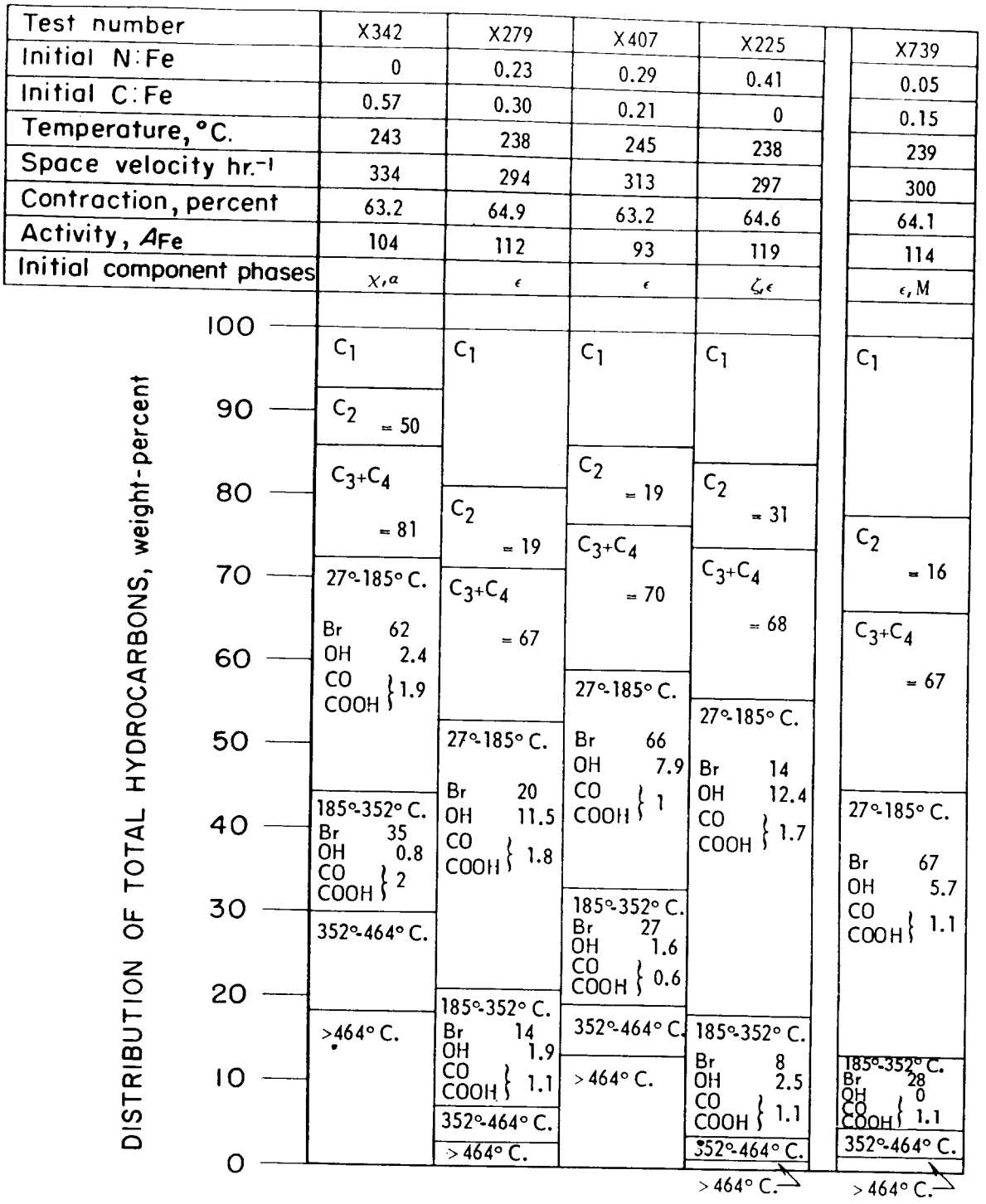

FIGURE 27.—Activity and Product Distribution From Carbonitrided Catalysts With $1H_2+1CO$ Gas at 21.4 Atmospheres. Total hydrocarbons includes oxygenated material dissolved in liquid phase.

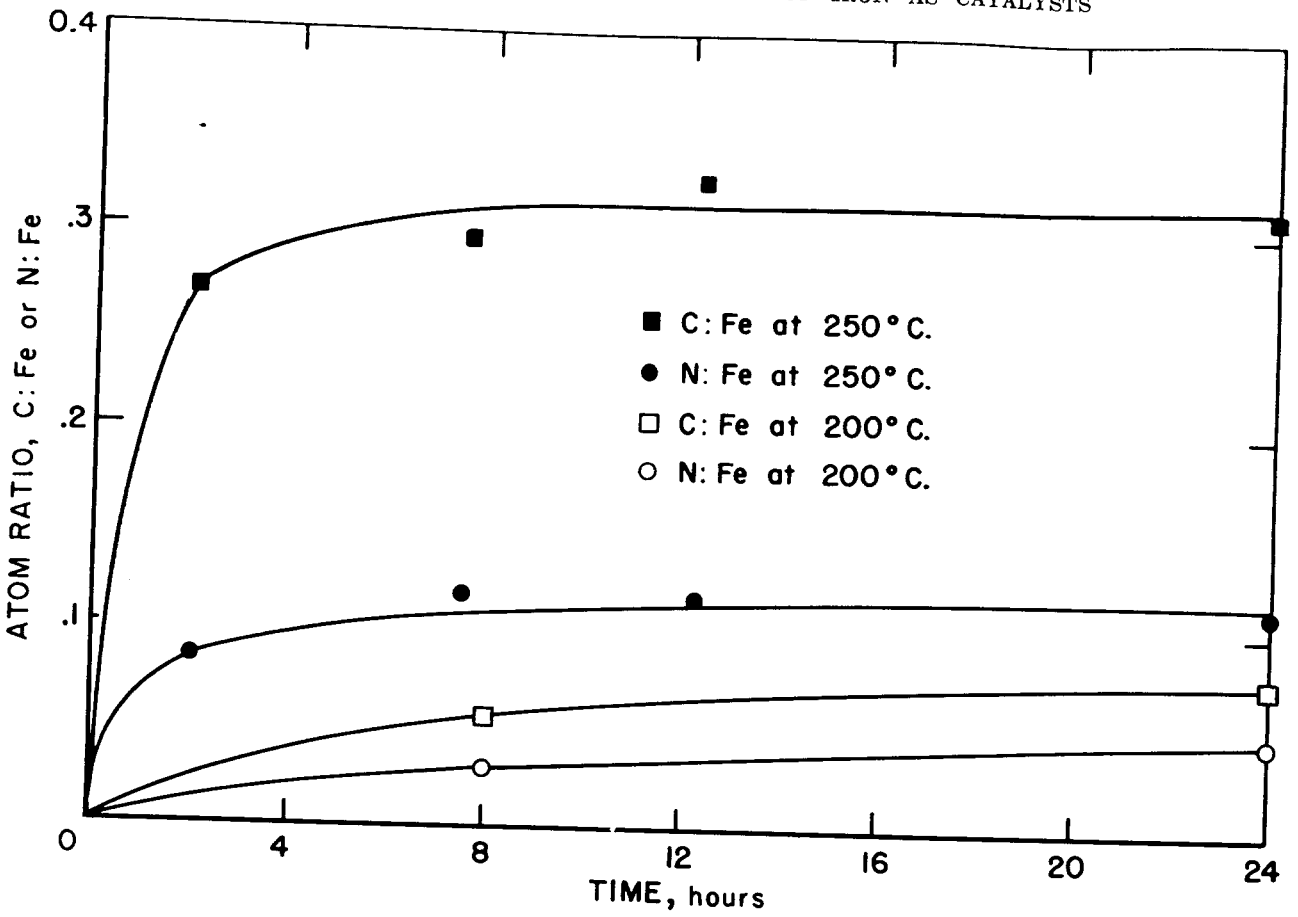

FIGURE 28.—Formation of ϵ-Iron Carbonitride on D3001 With Methylamine.

EXPLORATORY STUDIES ON PREPARATION OF IRON BORIDES

As iron forms interstitial borides similar in many respects to carbides and nitrides of iron, exploratory studies were made on preparation of catalysts containing iron borides. Iron borides can be prepared by dissolving boron in molten iron and cooling the resulting solution. For preparing catalysts this method cannot be used because the melts have surface areas that are too small. For this reason the same general procedure as used for preparing carbides and nitrides was employed; high surface area iron was treated with diborane (B_2H_6) or trimethyl boron $(CH_3)_3B$. These studies were made on 1- to 5-gram samples, and quantities of borided catalysts large enough for testing in the Fischer-Tropsch synthesis were never prepared.

The boriding procedures were too complicated to be considered practical for pretreating catalysts, and usually iron borides were only a minor phase in the final sample.

Diborane was prepared by the Schlesinger method (*69*), involving the reaction of lithium hydride with the ethyl etherate of boron trifluoride. As diborane reacts explosively with water vapor or oxygen, suitable precautions were taken to eliminate traces of air and moisture from the system used for preparing this compound and reacting it with catalyst samples. The purified diborane was stored in a 5-liter glass flask. Mixtures of 20 to 30 percent diborane in helium were prepared by passing helium over liquid diborane at −112° C., melting point of carbon disulfide.

In experiments using this mixture of about $1B_2H_6+3He$ on reduced and reduced and nitrided catalyst D3001, in an externally heated glass tube, no borides were formed in the temperature range from 150° to 300° C. (table 18), and the diborane was converted to higher boron hydrides that accumulated on the surface of the catalyst and glass reactor. Two of the samples were heated in an inert atmosphere at 450° to 500° C., and partial conversion of the iron to Fe_2B occurred. Attempts to prepare borides at 450° C. led to plugging of the reactor by the deposits of higher boron hydrides even though the concentration of diborane in helium had been decreased to less than 5 percent.

In a second series of tests a mixture of $1B_2H_6+99He$ prepared in a stainless steel cylinder was used, and the catalyst was heated by induction methods to insure that the catalyst temperature was greater than that of the reactor wall. In test B18 with nitrided D3001 (table 19), traces of Fe_2B were found after reaction at 400° C. Two alkali-free catalysts, fused Fe-Al_2O_3, P2007.2, and activated steel turnings, P1039, were also tried to determine whether the alkali inhibited boride formation. After annealing at 500° C. or above, moderately distinct X-ray-diffraction

TABLE 18.—*Boriding studies using a mixture of $1B_2H_6+3He$*

Catalyst	Treatment temperature, ° C.	Phases present (from X-ray diffraction)
D3001, reduced	200	α-Fe.
Do	250	α-Fe.
Do	150	α-Fe.
Do	[1] 200	α-Fe, Fe_2B.
D3001, nitrided	200	ε-Fe_2N (front half of bed).
Do	200	ε-Fe_2N, α-Fe (rear half of bed).
Do	300	ε-Fe_2N.

[1] Annealed 16 hours at 450° to 500° C.

TABLE 19.—*Boriding studies using a mixture of $1B_2H_6+99He$*

Sample No.	Catalyst	Diborane treatment temperature ° C.	Annealing temperature, ° C.	Phases present (from X-ray diffraction)
B14	D3001, reduced	200	500	α-Fe, Fe_2B.
B15-2	P2007.2, reduced	200	500	α-Fe, Fe_2B, Fe_3O_4.
B15-4	Same as B15-2		550	α-Fe, Fe_2B, Fe_3O_4.
B15-6	Same as B15-4		700–800	α-Fe, Fe_2B.
B15-8	Same as B15-6, extracted with HCl.			Fe_2B.
B17	P1039 steel turnings, oxidized, reduced.	200	550	Fe_2B, α-Fe.
B18-2A	D3001, reduced, nitrided.	400		α-Fe, γ′-Fe_4N, Fe_2B.
B18-2B	Same as B18-2A		550	α-Fe, Fe_2B.

patterns of Fe_2B as a minor phase were obtained. The sample in test B15–8 was extracted with a concentrated solution of hydrochloric acid. This treatment removed the α-iron in the sample, and a sharp diffraction pattern of Fe_2B was obtained on the residue.

These experiments suggest that diborane and higher borohydrides formed by its decomposition do not react with iron below 400° C., and that temperatures above 600° C. are required for formation of appreciable quantities of Fe_2B. The presence or absence of nitride or alkali in the catalysts makes little difference in the formation of borides. As temperatures above 600° C. are deleterious to reduced iron catalyst, this phase of the investigation was terminated.

Finally, several experiments were made in which reduced iron catalysts were treated with trimethyl boron. This compound was prepared by the reaction of methyl-magnesium bromide with boron trisulfide in *n*-butyl ether according to the method of Brown (*20*). A 1-percent mixture of trimethyl boron in helium from a stainless steel cylinder was passed over the catalyst. In tests at 500° C., iron boride, FeB, was produced as a minor phase.

STRUCTURAL AND CHEMICAL CHANGES IN CATALYSTS DURING PRETREATMENT AND SYNTHESIS

This section describes investigations on the pore geometry and phases present in iron Fischer-Tropsch catalysts during various stages of pretreatment and during synthesis. In the first and second parts surface areas and pore volumes are presented. These data provide a picture of the pore structure of the catalyst, which is required for a rational interpretation of the reaction. The third part presents electron- and X-ray-diffraction data for catalysts. These data are complementary, as X-ray diffraction provides information regarding the phases present in the entire particle, whereas electron diffraction detects only phases near the surface of crystallites.

STRUCTURAL CHANGES IN REDUCED-IRON CATALYSTS ON FORMATION OF OXIDE AND INTERSTITIAL PHASES

Although catalysts may sinter or otherwise change their physical structure in many catalytic processes (*9, 22, 33, 34, 64*) their chemical composition is seldom appreciably altered. When chemical changes do occur they usually have a marked effect on the process. The Fischer-Tropsch synthesis over initially reduced iron is one instance of a catalyst undergoing chemical change in the course of operation, namely reoxidation and carburization. Various authors (*16, 29, 55, 57, 80*) have attributed deactivation and short catalyst life to some of these reactions, and attempts have been made to find promoters and iron phases (*16, 75, 76*) that will catalyze the synthesis while resisting chemical changes. The present study deals with the physical changes accompanying the nitriding, carbiding, and reoxidation processes on a fused-iron catalyst of the synthetic-ammonia type (*43*).

Structural changes accompanying the initial reduction of this catalyst and its chemical changes during the synthesis have been described previously (*11, 43*). Kölbel and Engelhardt (*57*) have measured the rate of reoxidation of inducted iron catalysts with water vapor. The carbides and nitrides of iron have been extensively studied (*16, 25, 27, 31, 40, 52, 54, 60, 61*). Podgurski, Kummer, DeWitt, and Emmett (*68*) showed that little or no change in surface area occurred upon carbiding, while carbon monoxide chemisorption decreased tenfold to thirtyfold as the reaction progressed. Our exploratory experiments confirmed this work. The densities of the iron carbides and nitrides are known to be lower than the density of iron, but nowhere have the changes in catalyst structure been described as concurrent with formation of these phases or the oxide phase.

All experiments were carried out in glass tubes equipped with special four-way stopcocks (*4, 73*). To facilitate charging and removing the samples and to maintain the constant volume of the sample tube, the charging inlet was extended to the level of the stopcock and closed with a ground glass joint. After the tube was filled, a close-fitting glass rod was inserted into this inlet to minimize the dead space. These sample vessels were heated in a horizontal position in a small resistance furnace with automatic temperature control to $\pm 3°$ C. Changes in the samples were determined by weighing the entire tube on an analytical balance, and the loss or gain of oxygen, carbon, or nitrogen was calculated.

Dry electrolytic H_2, freed from traces of O_2 and H_2O vapor by passing over Cu heated to 350° C. and then over anhydrous $Mg(ClO_4)_2$, was used in the reductions. The 6- to 8-mesh catalyst of magnesia-potassium oxide promoted iron (D3001) had about 45 percent porosity [10] and an average pore diameter of about 800 A. when completely reduced at 550° C. (*43*). The oxidations [11] were carried out with prepurified (99.98-percent pure by mass spectrometer) nitrogen, which was saturated with freshly boiled distilled water by passing successively through pyrex sintered disc saturators at 40° C. and at room temperature (27° to 33° C.), respectively. Preparation of the nitrides has been described previously; anhydrous NH_3

[10] Percent porosity = 100(pore volume)/(particle volume by Hg displacement)

$$= 100(1 - \rho_{He}/\rho_{He}),$$

where ρ_{He} is density measured by displacement of mercury at atmospheric pressure, and ρ_{He} is density measured by displacement of helium.

[11] Available thermodynamic data (*36, 37, 80*) on oxidation of iron with water and carbon dioxide, the only oxidizing agents found in the tail gas of the Fischer-Tropsch synthesis, indicate that oxidation of metallic iron in bulk by carbon dioxide is unlikely under conditions in most of the catalyst bed. The equilibrium constant for the reduction of magnetite to α-Fe

$$K_1 = P_{CO_2}/P_{CO} \qquad (3)$$

ranges from 2.5 to 1.5 between 225° and 325° C., so that the partial pressure of carbon dioxide must be several times that of carbon monoxide for oxidation to take place. However, water vapor, either as a primary or as a final product of synthesis, is much more favorable for oxidation. The equilibrium constant for the reduction of magnetite,

$$K_2 = P_{H_2O}/P_{H_2} \qquad (4)$$

ranges from 0.019 to 0.058 in the same temperature range. Thus, only a small percentage of water vapor in the gas can oxidize the catalyst. Further, Almquist and Black (*2*) showed that appreciable amounts of oxygen were retained by an iron catalyst treated at 444° C. with $3H_2+1N_2$ gas containing only 0.016 percent of water vapor. Under these conditions the massive iron was not oxidized, but the amount of oxygen taken up was equivalent to oxidation of one iron atom in 400. Kölbel (*57*) found that an inducted, precipitated catalyst was completely reoxidized with $2N_2+1H_2O$ at 200° to 240° C. in 8 to 16 hours.

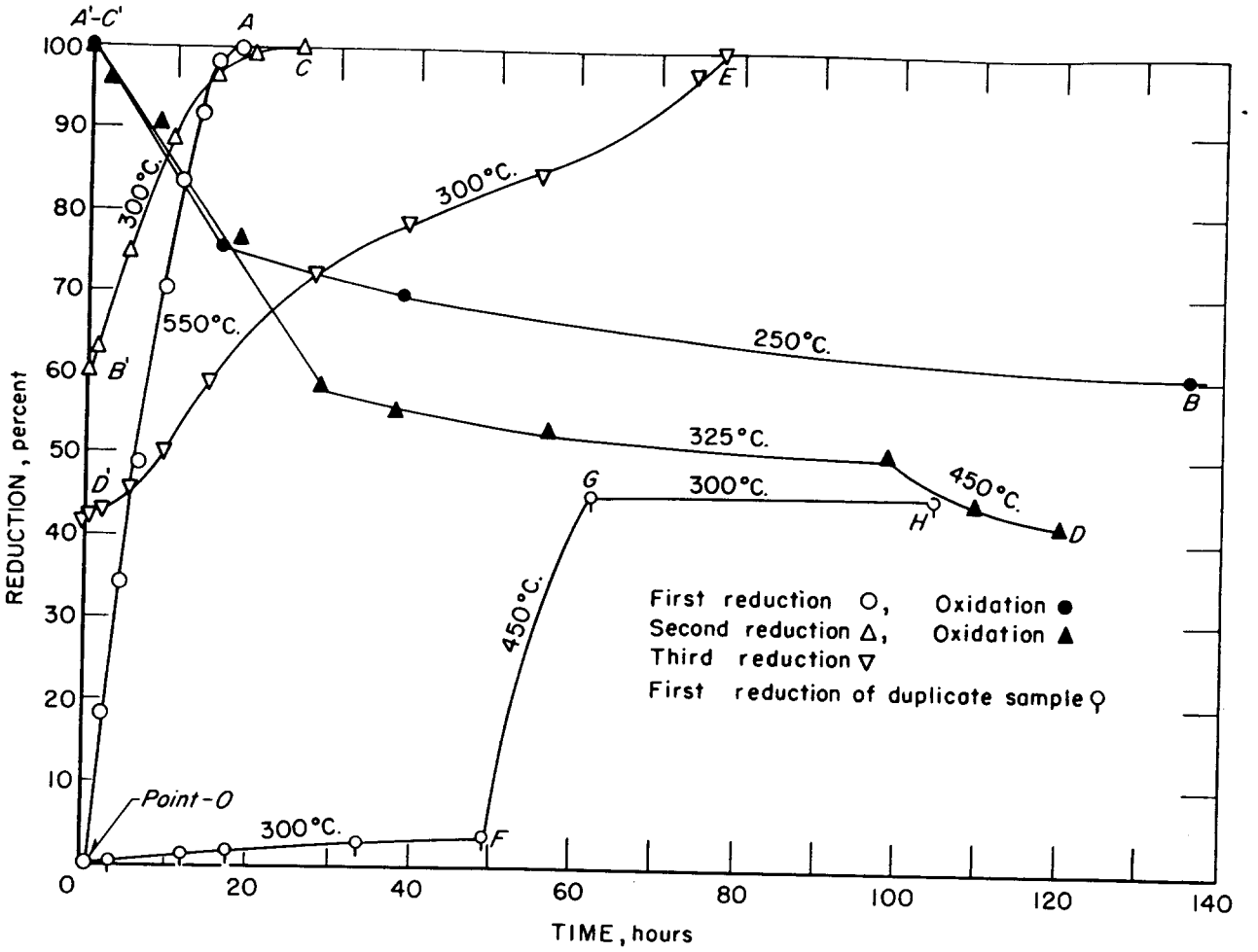

FIGURE 29.—Oxidation and Reduction of Fused-Iron Catalyst, D3001.

was used after further drying over fused potassium hydroxide. The hourly space velocity of the gas was 1,000 in reduction, oxidation, and nitriding.

Hägg carbide was prepared by treating the reduced catalyst with pure carbon monoxide at an hourly space velocity of 100. Carbiding was started at 150° C.. and the temperature was increased, as required to maintain the concentration of carbon dioxide in the exit gas at about 20 percent, to a maximum of 350° C. The exit gas was passed through a thermal conductivity gas-analysis apparatus, which controlled the rate of temperature increase of the electric furnace. Nearly pure Hägg carbide was formed in this way.

The methods for making the adsorption and density measurements have been described earlier (*7–9, 12, 43, 64*). All gases used for these measurements were analyzed with the mass spectrometer and found to be more than 99.8 percent pure. No wetting of the catalyst by mercury was observed. Surface areas were calculated from the V_m values obtained from the simple B.E.T. equation (*24*), using 16.2 A^2 as the cross-sectional area of the adsorbed nitrogen molecule.

Figure 29 shows the extent of reduction as a function of time during reduction and oxidation. The extent of reduction is defined as the weight of oxygen removed from the catalyst divided by the weight of oxygen associated with iron in the raw catalyst. After initial reduction with pure dry H_2 at 550° C. (curve *O–A*), the rate of oxidation of the catalyst at 250° C. with water vapor (*A'–B*) was rapid at first and then decreased to a low value. Re-reduction of the partly reoxidized catalyst at only 300° C. (*B'–C*) was almost as rapid as the initial reduction at 550° C. The sample was again oxidized (*C'–D*), this time at 325° C., with similar results. At the end of about 100 hours, the temperature was increased to 450° C. in an attempt to increase the rate of oxidation. An increase was observed, but this may have been caused by surface oxidation to hematite rather than by

TABLE 20.—*Adsorption measurements on reduced and reoxidized catalyst, D3001*

Gas	Treatment			Extent of reduction, percent	Surface area, $m.^2/g.$ of unreduced catalyst	V_m,[1] cc./g. (S.T.P.)	V_{co},[2] cc./g. (S.T.P.)	$\frac{V_{co}}{V_m}$	$\frac{\text{Area}^3}{f}$	$\frac{\text{Area}^3}{f^{1/2}}$
	Temperature, ° C.	Time, hours	Point on fig. 29							
H_2[4]			*O*	0	0	0	0			
N_2+H_2O	550	18	*A*	99. 7	4. 7	1. 07	[5](. 4)	[5](0. 4)	4. 7	4. 7
H_2	250	136	*B*	60. 4	2. 6	. 59	. 1	. 2	4. 3	3. 3
N_2+H_2O	300	27	*C*	100. 0	4. 5	1. 04	. 5	. 5	4. 5	4. 5
	325	98	*D*	42. 1	1. 7	. 39	. 04	. 1	4. 1	2. 6
	450	21. 5								
H_2[4]	550	19		99. 9						
N_2+H_2O	250	70	(6)	68. 4	2. 9	. 66			4. 2	3. 5
H_2[4]	550	18. 5	(6)	99. 8						
N_2+H_2O	250	66	(6)	68. 2	2. 8	. 64			4. 1	3. 4
H_2[4]	450	56		98. 0	8. 2	1. 88			8. 4	8. 3
	500	5								
N_2+H_2O	250	65		49. 8	3. 9	. 89			7. 8	5. 5

[1] Calculated by use of the simple B.E.T. equation (*24*). (Per gram of raw catalyst.)
[2] Difference between the N_2 and CO isotherms at −195° C. per gram of raw catalyst.
[3] f=extent of reduction, expressed as a fraction.
[4] Original reduction of raw catalyst.
[5] V_{CO}/V_m from previous work (*43*); V_{CO} was calculated using V_m for this sample.
[6] Density measurements were made on this sample.

bulk oxidation to magnetite, indicated by the reddish color of the catalyst. On re-reduction at 300° C. (*D'–E*), the rate of reduction was again much greater than that of the raw catalyst under the same conditions (*O–F*). After a raw sample had been reduced nearly 50 percent at 300° and 450° C. (*O–F–G*), it was again treated with hydrogen for about 40 hours more at 300° (*G–H*). These data show clearly that the reoxidized catalyst was much easier to reduce than the raw or the partly reduced catalyst.

Adsorption measurements made at the end of the various steps shown in figure 29 are given in table 20. In all cases the surface area decreased on reoxidation and increased to about its initial value when re-reduced. The chemisorption of carbon monoxide was sharply decreased by reoxidation; the ratios of $V_{CO}:V_m$[12] indicate that the relative amount of free iron on the surface of the reoxidized catalyst was less than half of the amount of the reduced catalyst. As the total surface area was decreased proportionally by reoxidation, the amount of iron (on the surface) available for oxidation was very small when the rate of reoxidation became low. The same behavior was observed for the sample initially reduced at 450° and 500° C. (table 20), except that the surface areas were about twice as large as those measured on the sample initially reduced at a higher temperature (*43*). The last two columns of table 20 are discussed later in this section.

[12] V_{CO} and V_m are the volumes of chemisorbed carbon monoxide and the nitrogen monolayer capacity in cubic centimeters (S.T.P.), respectively. The carbon monoxide chemisorbs only on the part of the surface that is iron (*23*). The ratio of $V_{CO}:V_m$, therefore, gives a measure of the fraction of the surface that is iron.

Structural data for various solid phases prepared from this catalyst are summarized in table 21, where the quantities used for comparing catalysts—volume of mercury displaced (V_{Hg}), pore volume, and surface area—are expressed per gram of unreduced catalyst. Thus, the reduced and reoxidized samples displaced the same volume of mercury as the raw sample, but the carbided and nitrided catalysts displaced 12 to 18 percent more (col. 5). On reduction, the catalyst developed nearly all its pore volume (col. 6), which decreased on reoxidation but increased enough on nitriding and carbiding to keep the percent porosity approximately constant (col. 8). The average pore diameters, calculated from the equation of Emmett and DeWitt (*35*), increased from that of the reduced catalyst, with both reoxidation and the formation of interstitial phases. The densities of the reoxidized catalysts agree almost exactly with those observed for the same catalyst at the same extent of reduction during its initial reduction (*43*).

The density of Fe_2N, calculated from the data of Eisenhut and Kaupp (*31*), is 7.02, compared to 6.82 from our data; thus, by assuming that the volumes of the phases present were additive, the density of our nitrided catalyst calculated from their data should be 6.50, compared to the observed 6.37. Similarly, according to Jack (*52, 54*) the density of Fe_2C is 7.20, compared to 6.77 calculated from our data.

Reactions of oxygen or water vapor with metals generally start with formation of a new phase at the surface. The oxide-metal interface

TABLE 21.—*Structural data as a function of solid phase in catalyst D3001* [1]

Treatment of catalyst	Phases present, X-ray analysis	Densities, g./cc.		V_{He}, cc./g. unreduced catalyst	Pore volume,[2] cc./g. unreduced catalyst	Pore volume, calculated from equation (6) in text, cc./g. unreduced catalyst	Porosity,[3] percent	Surface area, m.²/g. unreduced catalyst	Average pore diameter,[4] A
		Helium ρ_{He}	Mercury ρ_{Hg}						
None, raw	Fe_3O_4	4. 96	4. 91	0. 203	0. 002	0	1	0	
Reduced at 550°C	α-Fe	6. 95	3. 71	. 201	. 093	. 093	47	4. 7	785
Reoxidized [5] $f=0.684$.	α-Fe, Fe_3O_4	5. 94	4. 13	. 200	. 061	. 064	30	2. 9	820
Reoxidized [5] $f=0.682$		5. 93	4. 13	. 200	. 061	. 063	30	2. 8	860
Carbided [6]	χ-Fe_2C, α-Fe(?)	6. 28	3. 63	. 225	. 096		42	(7)	[7] (820)
Nitrided [8]	ϵ-Fe_2N	6. 37	3. 48	. 237	. 107		45	4. 8	898

[1] Except for the raw catalyst, all samples were reduced for 19 hours at 550° C. at a space velocity of 1,000 volumes H_2 per volume catalyst per hour.

[2] Pore volume is the difference of the volumes of mercury and helium displaced per gram of unreduced catalyst.

[3] Porosity=100×pore volume per mercury volume.

[4] $d=4\times$pore volume per surface area (*55*).

[5] Density measurements were made on this sample. f=extent of reduction.

[6] Atom ratio, C:Fe=0.494.

[7] Surface area not determined; several other samples showed no change in surface area with carbiding for this catalyst; see also reference (*68*). The surface area was assumed unchanged, and the pore diameter was calculated on this basis.

[8] Atom ratio, N:Fe=0.482.

moves into the metal either by diffusion of oxygen into the metal or metal diffusing through the oxide layer. The work of Evans (*38*) indicates that, after magnetite forms an interface on the iron surface, the oxide grows by migration of iron through the oxide layer. Thus the rate of reoxidation decreases rapidly as the oxide layer is formed, and the rate eventually approaches the rate of diffusion of iron through the oxide layer. The reduction of this oxide layer is more rapid than the initial reduction, because the reoxidized catalyst has a larger surface area than the raw catalyst. By this mechanism oxide can form in the pores without expanding the pore system and increasing the volume of mercury displaced by the catalyst. All the results can thus be explained qualitatively. To account quantitatively for the observed changes in surface area (table 20), however, it is necessary to consider the geometrical changes in the pores themselves. Two limiting cases are considered: (1) The pore volume decreases by decreasing the total length of pores of constant average diameter. (2) The pores maintain their length, but their diameters decrease as the reaction proceeds.

In the first case since length is the only variable

$$A_x/A_R=L_x/L_R, \tag{5}$$

where A and L are the area and total length of pores, respectively, per gram of unreduced catalyst, and the subscripts x and R refer to the partly reduced or oxidized catalyst and the completely reduced catalyst, respectively. The pore volumes V_x and V_R, also per gram of unreduced catalyst, can be expressed in terms of the initial and final volumes, V_o and V_F, of the catalyst, and of the extent of reduction, f (*43*),

$$V_x=(V_o-V_F)f=V_Rf. \tag{6}$$

Equation (6) requires only that the volume of mercury displaced by a gram of unreduced material does not change on reduction. As this condition is fulfilled for the reoxidized catalyst also, equation (6) may be used to relate the surface area to the extent of reduction. Thus, from equations (5) and (6)

$$\frac{A_x}{A_R}=\frac{L_x}{L_R}=\frac{V_x}{V_R}=f, \tag{7}$$

and $A_x/f=A_R$. As shown in column 10 of table 20, the ratio is about 10 percent low for the reoxidized catalyst. This is an upper limit because the effects of thermal sintering are superimposed on the results.

The same sort of treatment was applied to the second limiting case, yielding

$$\frac{A_x}{A_R}=\frac{d_x}{d_R}=\left(\frac{V_x}{V_R}\right)^{\frac{1}{2}}=f^{\frac{1}{2}}. \tag{8}$$

By equation (8), $A_x/f^{\frac{1}{2}}=A_R$. This ratio is about 25 to 30 percent too low (col. 11, of table 20).

Thus, while neither mechanism is in good agreement with experiment, the second postulate is worse than the first. It is rather surprising that both postulates give low results; the most logical explanation, a combination of the two effects, is precluded because it would necessarily give intermediate (low) results. Three plausible explanations for the observed surface areas being smaller than those predicted by the two simplified mechanisms may be suggested: (1) The smaller pores are preferentially and more or less completely filled with oxide. (2) Some of the pores have developed bottlenecks, that is, become partly plugged with oxide, so that they are permeable to helium at 30° C., but impermeable to nitrogen at −195° C. (3) The pore walls, originally rough, become smoother as the reoxidation proceeds.

Available data are inadequate to differentiate between these possibilities. The first two ways seem improbable because, in a real system, complete blocking of a fraction of the pores would be expected. This would be accompanied by an excessive decrease in the helium density, which is not observed. An inconclusive attempt was made to prove the presence of constrictions by studying the hysteresis of the nitrogen adsorption isotherms at −195° C.[13] The last possibility has several points in its favor, although there is little direct evidence to support it. This catalyst developed average pore diameters ranging from 330 to 2,400 Å., while the temperature of the reduction was increased from 450° to 650° C. (*43*). This effect was almost entirely due to change in surface area, rather than in pore volume. Further, a catalyst reduced completely at 450° C., when heat-treated in helium for 16 hours at 550° C., had the same pore diameter as that of the 550° C. reduction. McCartney and Anderson (*62*) made electron micrographs of replicas stripped from a polished surface of this catalyst after reduction at 450° and 550° C. While these showed pore openings that compared reasonably well with the pore diameters previously calculated from the surface area-pore volume data (*64*), no definite differences were observed in the dimensions of the replica structure from samples reduced at the two temperatures. By tacitly assuming the same roughness factor for the pore walls formed at all temperatures, the earlier results required that one pore system change as the reduction temperature increased and be replaced by a new one with a smaller number (or total length) of pores of a larger diameter. A simple explanation of these data is that the pore walls originally are rough and thus yield low values for the pore diameter. As the temperature is increased, these walls smooth out, giving an apparent increase in the pore diameter. This example illustrates the danger involved in putting too much credence in the exact value of the pore diameters calculated from the Emmett-DeWitt equation (*35*); at the same time it offers a possible explanation of our data.

The changes in structure that occur concurrently with formation of the interstitial carbides and nitrides are much easier to interpret. As the metal lattice expands, the pore volume increases, but the surface area changes only slightly if at all. Consequently, the average pore diameter increases, but the porosity remains constant. This is the behavior of an expanding matrix. If a solid containing a hole is expanded, the apparent volume, pore volume, and pore diameter increase, the surface area increases only slightly, and the percent porosity remains essentially constant. The available data fit this simple picture.

STRUCTURAL CHANGES OF IRON CATALYSTS DURING PRETREATMENT AND SNYTHESIS

In this section structural changes occurring in iron catalysts during pretreatment and synthesis are described and related to the results reported in the previous section (*78*).

For iron catalysts structural changes during synthesis are more complex than for cobalt catalysts. Studies of a used cobalt catalyst (*9*) have shown that while the total volume of the catalyst does not change during synthesis, sizable decreases in the surface area and pore volume occur. These decreases are attributed to the accumulation of waxy products in the pores of the catalyst. On removing the wax by a simple hydrogen treatment the original porous structure of the catalyst was regained. Carbiding or oxidation of the cobalt does not occur, nor are appreciable amounts of elemental carbon deposited. With iron catalysts, elemental carbon is deposited as well as wax, and most of the iron is converted to carbides and magnetite. The present section reports structural data obtained from two types of iron catalysts after they had been operated in the synthesis.

Two different types of iron catalysts were investigated—a precipitated iron oxide, copper oxide, potassium carbonate catalyst, P3003.24; and a fused-iron oxide, magnesium oxide, potassium oxide catalyst, D3001. Preparation, composition, and structural information pertaining

[13] The hysteresis loop of the nitrogen isotherm of the reoxidized catalysts seemed to be enlarged near the vapor pressure of nitrogen, P_o, but P_o had shifted to a value about 10 mm. greater than that of the gas-filled tube without catalyst. Mass spectrometric analysis of nitrogen in the system showed that the only impurity was 0.005 percent argon. These observations were reproducible but cannot, at present, be explained.

to these catalysts have been described in the previous section, and in the appendix.

Catalyst P3003.24 was inducted in a catalyst testing unit at atmospheric pressure for 24 hours with $1H_2+1CO$ gas at 230° C. and operated (*11, 16, 79*) for about 7 weeks at an average temperature of 221° C. and a pressure of 7.8 atmospheres. A reduced sample of D3001 was operated for 2 weeks at 253° C. and a pressure of 21.4 atmospheres, and a nitrided sample of the same catalyst was operated for 6 weeks at 249° C. and 21.4 atmospheres. All of the catalyst tests were made with $1H_2+1CO$ synthesis gas and demonstrated typical activities (*13, 16, 76*) for these types of materials.

At the end of each synthesis experiment the catalyst was cooled to room temperature in the reactor by flowing nitrogen over the catalyst bed. The catalyst was then dropped into a glass jar, which was continuously flushed with carbon dioxide. To prevent atmospheric oxidation, all subsequent handling and transfer of the catalyst was done in carbon dioxide.

Surface area and pore volume measurements were made on three samples of each used catalyst. The first was a sample of the catalyst as removed from the reactor. The second was extracted with boiling toluene in a modified Soxhlet apparatus (*63*) for about 2 days. This treatment removed essentially all of the waxy reaction products from the catalyst. The third sample was extracted in the same manner as the second and then was reduced with hydrogen.

All adsorption and density determinations were carried out in pyrex tubes equipped with special four-way stopcocks (*4, 44*). The method used for obtaining pore volumes from mercury and helium densities was that described previously (*12*). Surface areas were calculated from nitrogen adsorption data using the simple B.E.T. equation (*24*) with 16.2 A^2 (*43*) taken as the cross-sectional area of the adsorbed nitrogen molecule. Chemical analyses were made on each catalyst sample by conventional methods. The amount of oxygen present was not determined directly, but was calculated by difference.

Comparison of the structural changes in the used catalysts may be conveniently made by studying the histograms shown in the following three figures (30–32). The total volume of the catalyst (volume of solids plus pores), indicated by displacement of mercury, is shown by the total histogram. The shaded area represents the true volume of the catalyst (volume of solids only) indicated by displacement of helium. The open area is the pore volume, that is, the difference between the displacement of mercury and the displacement of helium. The numbers in the histogram following the letters $\overline{C}$, $\overline{O}$, or $\overline{N}$ represent the atom ratios in the catalysts of carbon to iron, oxygen to iron, and nitrogen to iron, respectively. At the top of the histograms the surface areas and the average pore diameters [14] are tabulated. All values of areas and volumes are per gram of unreduced catalyst.

Structural data for catalyst P3003.24 are presented in figure 30 and table 22. The raw catalyst is principally a ferric oxide gel having a large surface area. Reduction of the ferric oxide to magnetite with hydrogen saturated with water vapor, or reduction to iron with dry hydrogen, caused a drastic decrease in the surface area (*43*). The total volume of the catalyst was likewise decreased, the decrease being more pronounced upon reduction to iron. After induction [15] and use in the synthesis, the catalyst had virtually no surface area or pore volume, indicating that the pores had been

[14] Computed from the equation $d=4V/A$, where V is the pore volume and A is the surface area.

[15] An activation treatment with $1H_2+1CO$ gas before synthesis. The ferric oxide gel is reduced to Fe_3O_4, and part of the iron is converted to higher iron carbides.

TABLE 22.—*Structural data for precipitated catalyst, P3003.24,* Fe_2O_3–CuO–K_2CO_3

Treatment [1]	Phases present X-ray analysis	Densities, g./cc.		Surface area m.²/g. unreduced catalyst	Pore volume, cc./g. unreduced catalyst	Volume Hg displaced, cc./g. unreduced catalyst	Average pore diameter, A.
		Helium ρ_{He}	Mercury ρ_{Hg}				
None, raw	Amorphous	4. 43	2. 83	184	0. 125	0. 347	27
R	α-Fe, Cu	7. 60	2. 73	6. 3	. 155	. 247	968
R', H_2+H_2O	Fe_3O_4, Cu	5. 25	2. 75	11. 3	. 151	. 317	536
IU	Fe_3O_4	3. 06	3. 10	. 1	. 000	. 320	----------
IUE	Fe_3O_4	4. 51	2. 76	11. 7	. 123	. 319	420
IUER''	α-Fe, Fe_3O_4, Cu	5. 50	2. 73	7. 8	. 140	. 279	718

[1] *R*=reduced with H_2 at 300° C., *R'*=reduced to Fe_3O_4 with H_2+H_2O at 250° C., *I*=inducted with $1H_2+1CO$ at 230° C., *U*=used, *E*=extracted with boiling toluene, *R''*=reduced with H_2 at 300° C.

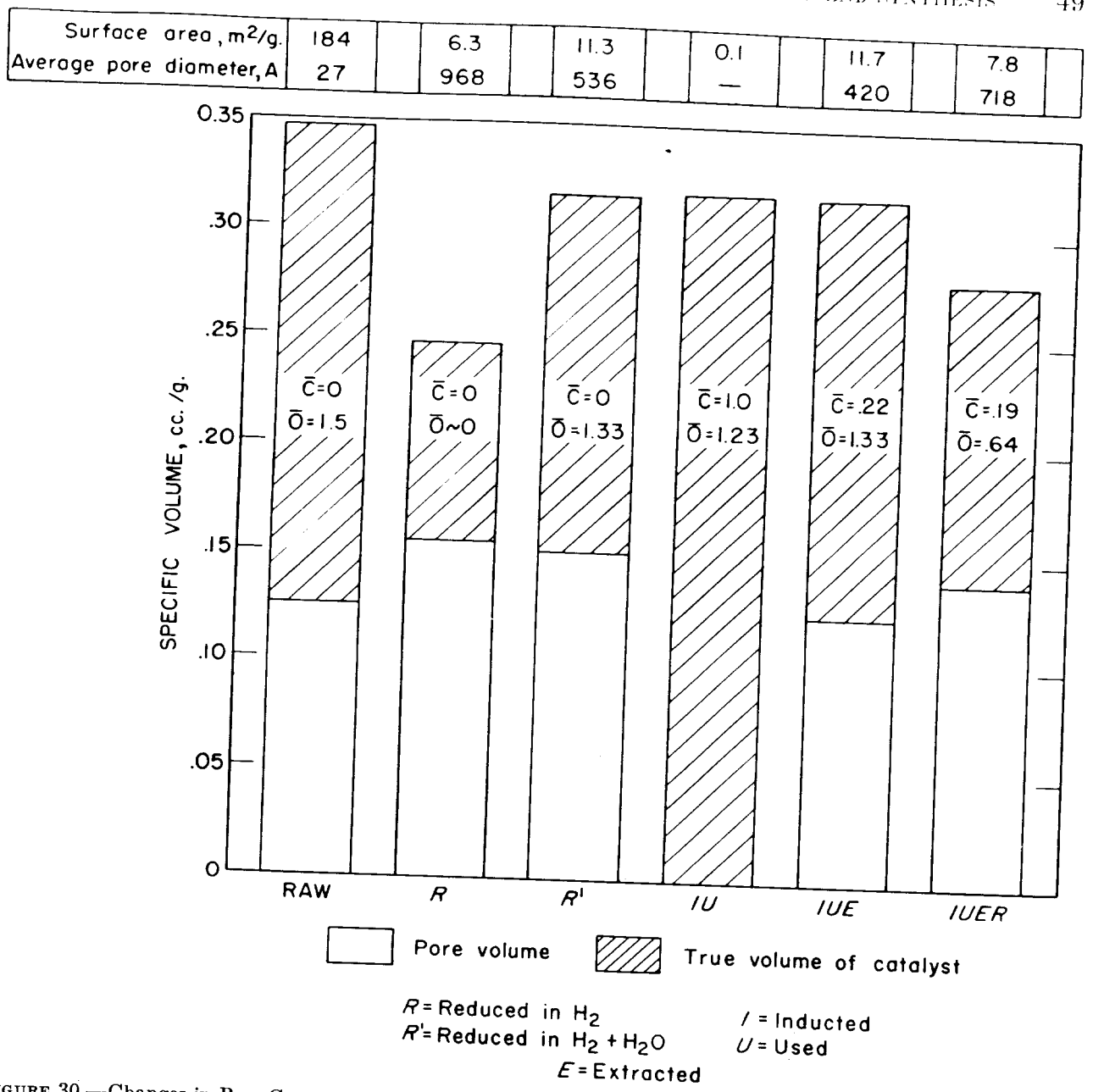

FIGURE 30.—Changes in Pore Geometry and Composition of Precipitated Catalyst, P3003.24, in Pretreatment and Synthesis.

almost completely filled with wax. After extracting the wax with toluene, the surface area and pore volume of the catalyst increased appreciably. Partial reduction of the extracted catalyst resulted in a moderate decrease in surface area and a slight increase in the pore volume, approaching the values for the completely reduced sample. The total volumes of used and extracted portions remained about the same as the volume of the sample reduced to magnetite. Reduction of the used catalyst caused a slight decrease in total volume.

In figure 31 and table 23 structural data for the fused-iron catalyst D3001 are presented. The raw catalyst had no pore volume or surface area but upon reduction porosity increased to about 40 percent, and the area increased to 9.4 m.²/g. On partial reoxidation the surface area (table 21) and pore volume both decreased. However, the volume of mercury displaced by the catalyst was unchanged in the reduction or the subsequent oxidation. This behavior has been demonstrated in this laboratory previously (*43*), and Westrik and Zwietering (*87*) have also shown that a single crystal of magnetite does not change its shape or dimensions during reduction. When the reduced catalyst was converted to Hägg carbide by treatment

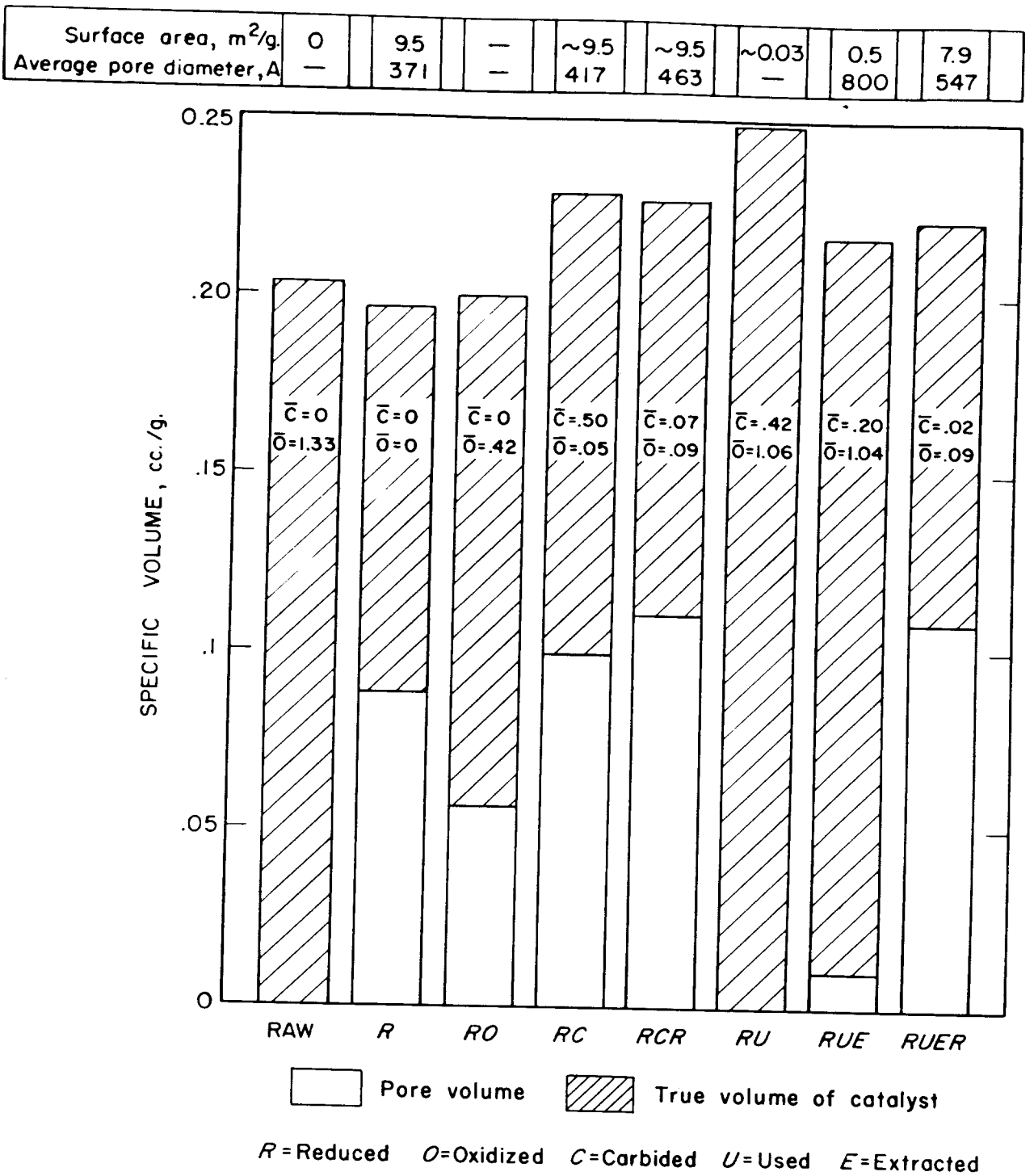

FIGURE 31.—Change in Pore Geometry and Composition of Fused Catalyst, D3001, in Carbiding and Synthesis.

with carbon monoxide, both the pore volume and the volume of mercury displaced were increased, suggesting that the carbon had entered into the arrays of iron atoms, increasing the size of the matrix forming the pore system. This behavior is quite different from the oxidation of the catalyst, when the oxygen apparently entered and filled the pores that were available in the reduced catalyst. Reduction of the carbided catalyst in hydrogen at 450° C. removed most of the carbon from the catalyst. However, the total volume of the catalyst did not return to the original value of about 0.20 cc./g.

TABLE 23.—*Structural data for fused catalyst D3001, reduced*

Treatment [1]	Phases present X-ray analysis	Densities, g./cc.		Surface area m.²/g. unreduced catalyst	Pore volume, cc./g. unreduced catalyst	Volume Hg displaced, cc./g. unreduced catalyst	Average pore diameter, A
		Helium ρ_{He}	Mercury ρ_{Hg}				
None, raw	Fe_3O_4	4. 96	4. 91	0	0. 002	0. 203	
R	α-Fe	6. 82	3. 78	9. 5	. 088	. 197	371
RO	α-Fe, Fe_3O_4	5. 94	4. 13	[2]	. 061	. 200	[2]
RC	χ-Fe_2C	6. 38	3. 60	[3] (9. 5)	. 099	. 229	417
RCR	α-Fe	6. 58	3. 38	[3] (9. 5)	. 110	. 227	463
RU	Fe_3O_4, α-Fe	4. 06	4. 06	~. 03	. 000	. 249	
RUE	Fe_3O_4, α-Fe	4. 69	4. 48	. 5	. 010	. 217	800
RUER	α-Fe, Fe_3O_4	6. 68	3. 44	7. 9	. 108	. 222	547

[1] *R*=reduced with H_2 at 450° C.; *O*=oxidized with N_2+H_2O at 250° C.; *C*=carbided with CO at 180° to 340° C.; *U*=used; *E*=extracted with toluene.

[2] Not determined.

[3] Not determined, but measurements on other samples have shown that surface area does not change appreciably during carbiding.

TABLE 24.—*Structural data for fused catalyst, D3001, nitrided*

Treatment [1]	Phases present X-ray analysis	Densities, g./cc.		Surface area m.²/g. unreduced catalyst	Pore volume, cc./g. unreduced catalyst	Volume Hg displaced, cc./g. unreduced catalyst	Average pore diameter, A
		Helium ρ_{He}	Mercury ρ_{Hg}				
None, raw	Fe_3O_4	4. 96	4. 91	0	0. 002	0. 203	
R	α-Fe	6. 95	3. 71	4. 1	. 094	. 201	917
RN	ε-Fe_2N, γ'-Fe_4N	6. 39	3. 49	4. 0	. 104	. 231	1, 040
RNR'	α-Fe	7. 08	3. 75	4. 1	. 092	. 196	898
RNO, Ō=0. 22	ε-Fe_2N, Fe_3O_4	6. 23	3. 62	3. 9	. 093	. 229	954
RNOR''	α-Fe	7. 04	3. 48	4. 1	. 107	. 211	1, 040
RNO', Ō=0. 81	Fe_3O_4, ε-Fe_2N, γ'-Fe_4N.	5. 09	4. 01	1. 8	. 049	. 229	1, 090
RNO'R''	α-Fe	6. 71	3. 33	4. 8	. 113	. 225	942
RNU	ε-Fe_2X,[2] Fe_3O_4, $FeCO_3$.	3. 98	3. 91	. 4	. 005	. 249	500
RNUE	ε-Fe_2X, Fe_3O_4, $FeCO_3$	5. 00	3. 98	4. 6	. 046	. 228	400
RNUER'''	α-Fe, Fe_3C	6. 93	3. 51	7. 5	. 109	. 220	580

[1] *R*=reduced with H_2 at 550° C.; *N*=nitrided with NH_3 at 350° C.; *R'*=reduced with H_2 at 300° C.; *O*=oxidized with N_2+H_2O at 250° C.; *R''*=reduced with H_2 at 450° C.; *O'*=oxidized with N_2+H_2O at 350° C.; *U*=used; *E*=extracted with toluene; *R'''*=reduce in H_2 at 400° C.

[2] Iron carbonitride.

After the catalyst had been used in the synthesis, the total volume had increased to about 0.25 cc./g. The pore volume and surface area were essentially zero, because the pore volume was decreased by both wax in the pores and oxidation. Extraction of this catalyst with boiling toluene increased the pore volume and surface area slightly and decreased the total volume of the catalyst particles. This may be interpreted as removal of wax from the external surface of the particle as well as from the pores. The final histogram represents the pore geometry of the used catalyst after extraction and after reduction at 450° C. Here the pore volume and total volume of the particle were similar to those observed for the reduced, carbided, and reduced catalyst. The total volume of the reduced, used, extracted, and reduced catalyst was about 13 percent higher than that of the original reduced catalyst.

Figure 32 and table 24 show a similar series of tests on fused, nitrided iron catalysts. In this series the original reduction was done at 550° C. rather than 450° C. This increased reduction temperature resulted in a catalyst having a smaller surface area and a larger average pore diameter. After nitriding, the total volume and pore volume of the catalyst were appreciably increased, as shown on the third histogram. However, when the nitrogen was removed by hydrogenation the catalyst properties again were those of the reduced catalyst; the nitrogen apparently was removed completely and did not stabilize the expanded structure as observed with carbided catalysts. Partial oxidation of the nitrided catalyst resulted

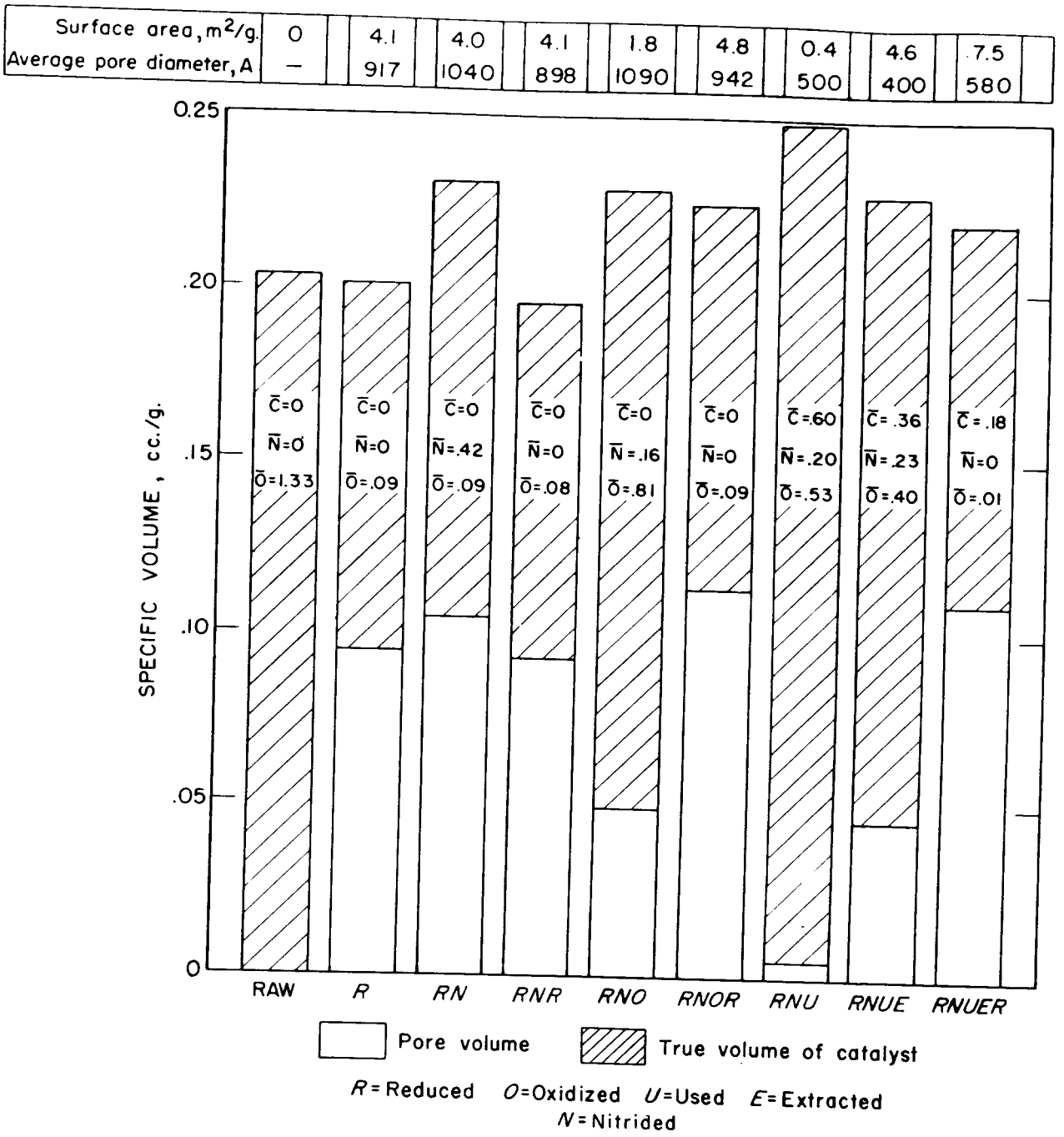

FIGURE 32.—Changes in Pore Geometry and Composition of Fused Catalyst, D3001, in Nitriding and Synthesis.

in a considerable decrease in the surface area and pore volume, shown in the fifth histogram. Total volume remained about the same. Oxidation of a nitrided catalyst was much more difficult than oxidation of a reduced catalyst. The nitrides designated by the fifth and sixth histograms were oxidized at a temperature of 350° C., compared with 250° C. for the reduced catalysts (*44*). After reduction of the nitrided, oxidized catalyst, the pore volumes were larger than the pore volume of the reduced, nitrided, and reduced catalyst. The total volume decreased slightly and was almost the same as that of the original nitride. Oxidation of the nitride, therefore, had a stabilizing effect on the expanded structure.

After 6 weeks of synthesis, the seventh histogram, the nitrided, used catalyst had only a very small pore volume and displaced a greater amount of mercury than the reduced or even

the reduced, nitrided catalyst. Its surface area was relatively low but appreciable. After extraction in toluene the pore volume was increased, and the volume of mercury displaced by the catalyst was decreased. Accompanying this change was a large increase in the surface area of the catalyst. Finally after reduction in hydrogen at 400° C. the nitrogen was removed completely, but the carbon remained in moderate amounts in the catalyst. The surface area was significantly increased, and the volume of mercury displaced by the catalyst was larger than that of the original reduced catalyst. Here again the amount of carbon remaining, or the intermediate formation of oxide, apparently was sufficient to stabilize the expanded structure.

Changes in a precipitated-iron catalyst during synthesis are relatively minor. The induction procedure, usually preceding synthesis, largely destroys the gel structure of the raw material and results in a catalyst that is essentially magnetite and iron carbide. This inducted catalyst, although of low mechanical strength, is apparently quite stable during synthesis—shown by the fact that after extraction to remove waxes, the used catalyst is very similar to the starting material in both chemical composition and physical structure.

However, reduced- or nitrided-fused catalysts undergo major changes in surface area and pore volume during synthesis. Here the structure and composition are affected by several reactions that probably occur simultaneously. To summarize the structural changes of fused-iron catalysts that occur during pretreatment and synthesis, let us consider briefly what happens to the catalyst during each of the following procedures:

1. *Reduction.*—During reduction no change takes place in the total volume of the catalyst, but a pore structure is generated by removing oxygen (*43*). This process occurs with pure magnetite, but the presence of structural promoters greatly assists in maintaining a pore structure of moderate surface area. It is probably not necessary to postulate a framework of structural promoter that is continuous throughout the structure. Thus crystallites of structural promoter may be considered as bricks in a wall of reduced catalyst.

2. *Reoxidation.*—Oxidation of a reduced catalyst is rapid initially, but the rate decreases very quickly with time or extent of oxidation (*44*). The reaction proceeds at the internal surface and the layer of oxide progressively thickens and quickly smooths out the surface, thus decreasing the pore volume and surface area. This reoxidation process occurs on a solid framework of iron and promoter crystallites that maintain the total volume of the catalyst constant.

3. *Nitriding and Carbiding.*—During these procedures the metal crystallites expand, the observed increase in the total volume being about 13 percent for carbides and about 17 percent for nitrides. The pore volume and average pore diameter increase, but the surface area changes only slightly.

4. *Reduction of Nitride.*—When iron nitride is reduced with hydrogen, the metal contracts to its original volume. Although this process is largely reversible, it does lead to disintegration of some of the catalyst particles. Differential expansion and movement about the structural promoter aggregates may be responsible for the breakup.

5. *Oxidation of Nitride.*—During the oxidation of iron nitride with steam, nitrogen is displaced only from the part of the catalyst that is oxidized. Hydrogen formed during the steam oxidation is apparently ineffective for reducing the nitride in the presence of water vapor. Thus, the oxide is built on a substrate of nitride.

6. *Reduction of Oxidized Nitride.*—In this step both the oxide and the nitride are reduced to metallic iron. The oxide portion will retain the bulk volume of the original nitride, and the nitride will attempt to revert to the volume of the original reduced catalyst. The relative amounts of oxide and nitride will then determine the final total volume of the catalyst. The oxide may be considered as a layer of cement over the nitride. If this oxide layer is sufficiently thick, it will prevent overall shrinkage of the catalyst particle during reduction.

7. *Reduction of Carbide.*—Apparently some free carbon is produced during carburization as well as in subsequent hydrogenation, and some oxide is formed in carburization. In addition, carbidic carbon is probably not completely removed during reduction of the carbide with hydrogen. The presence of carbon in the catalyst after reduction prevents the solid from regaining its original density; that is, carbon aggregates between the crystallites may prevent the return of the overall structure to its original state. Oxidation of iron carbide is probably similar to oxidation of the nitride; the oxide layer is probably built on a substrate of carbide.

Thus, physical and chemical changes in an iron catalyst during synthesis are quite extensive. Reduced catalysts oxidize considerably and carbides are formed. Nitrides oxidize to a smaller extent than reduced catalysts, but they are largely converted to carbonitrides. The active portion of the catalyst is probably confined to a thin zone or shell on the external surface of the particles (*13*). The low surface areas obtained for the used catalyst in figure 31 confirm the fact that only a small fraction of the total surface area of the catalyst is required to maintain the synthesis reaction. The inner part of the catalyst then may be considered to be inert, but it is important in that it provides a mechanically stable substrate for the active zone.

ELECTRON- AND X-RAY-DIFFRACTION STUDIES OF IRON FISCHER-TROPSCH CATALYSTS

Electron-diffraction patterns were determined on a number of iron catalysts after pretreatment and synthesis, and these patterns have been compare with those obtained from X-ray diffraction. The catalyst particles used were crushed to obtain the finely divided material required for diffraction examination, and the electron-diffraction data show the crystalline phases present near the external surface of

these fine particles; X-ray-diffraction data show the phases in the entire sample (*63*).

Electron diffraction has been frequently mentioned as an excellent method for studying solid catalysts. The electrons usually penetrate less than 0.1 micron and hence the diffraction pattern results from the crystal structure of the solid within about 1,000 A. of the surface. However, almost all of the published work on electron diffraction by catalysts has been on those of the evaporated film type (*17*), not on the granular or powdered types used in commercial processes.

X-ray analysis yields diffraction patterns resulting from both surface and bulk phases since X-rays penetrate solids. However, the phases near the surface of a heterogeneous solid may comprise only a small fraction of the solid and may therefore not be detectable by X-ray diffraction analysis. X-ray analysis and electron diffraction are thus complementary. Both types of diffraction patterns result from diffraction by crystallites larger than about 30 A. in diameter. In both cases the degree of order within the crystallite and its size are important in determining the completeness and the sharpness of the resulting diffraction pattern.[16] The present diffraction study was made with iron Fischer-Tropsch catalysts after various pretreatments and use in the synthesis.

The compositions and methods of preparing and testing catalysts used in this study are described in the appendix. Procedures for pretreating catalysts have been given.

X-ray-diffraction methods were essentially the same as those previously described (*50*). Used-catalyst samples, wet with hydrocarbons, were ground to about 120-mesh in either a simple mortar or a Plattner's diamond mortar, depending on hardness and malleability. Wet samples were mixed with collodion, packed in 19-gauge stainless steel tubes of 0.7 mm., inside diameter, and extruded. These procedures avoided oxidation detectable by X-ray diffraction.

To obtain satisfactory transmission-electron-diffraction patterns of solids, the particles must be very fine since electrons can penetrate only a very thin layer of material before they are inelastically scattered and incapable of contributing to the diffraction rings. For 60-kv. electrons the greater part of the diffraction pattern is formed by electrons that have penetrated not more than 0.1 micron of materials as dense as metals (*82*). The particles need not be as small as this, because diffraction can occur through protrusions on and around the periphery of larger particles. However, the smaller the average size of the particles, the greater will be the amount of material that is sufficiently thin to contribute to the diffraction pattern.

The precipitated catalysts were easily ground to very fine particles, but the fused catalysts were much harder, often necessitating rigorous and prolonged grinding in a synthetic sapphire mortar. The catalysts were covered by liquid toluene or heptane during this operation to prevent oxidation. Several drops of concentrated slurry were then placed on a microscope slide, about four drops of a 2-percent solution of Parlodion in amyl acetate were added, and the slurry was mulled with a glass rod to disperse the particles. More amyl acetate was added until the material appeared well dispersed. A little of the slurry adhering to the rod was then quickly drawn out on a clean slide, leaving upon drying a dispersion of particles embedded in a Parlodion film. This was scored into ¼-inch squares and floated off on a water surface. Two superimposed ⅛-inch discs of 200-mesh screen were brought up under one of the squares that appeared of suitable density, and the screens and film were lifted out and blotted on cloth. The top screen was then lifted off, and the sample was ready for examination.

The diffraction patterns were obtained with the diffraction adapter of an RCA Model B electron microscope, using 60-kv. electrons. They were photographed on lantern slide medium plates with exposures of about 1 minute. The instrument was calibrated by measuring the diffraction rings of magnesium oxide smoke. The d values of these were taken from the tables of Hanawalt, Rinn, and Frevel (*45*). The formula $d/n=K'/D$, derived from the Bragg diffraction equation, for fixed accelerating voltage (λ of electrons) and fixed specimen-to-plate distance was used to calculate the interplanar spacings, d, from the diameter of the rings, D, after determining K' with the calibrating material (*66*).

The first electron-diffraction patterns of used iron catalysts showed only adsorbed wax, the patterns being identical with those obtained from the Fischer-Tropsch wax alone. Extraction of the catalysts with toluene for 48 hours in a modified Soxhlet apparatus was sufficient to greatly reduce or to eliminate the diffraction lines corresponding to wax. Based on these preliminary experiments the following method

[16] An incorrect but widely held view is that the electron-diffraction patterns of finely divided, nearly amorphous material will give sharp, easily identifiable patterns, while X-ray-diffraction patterns of the same sample may be diffuse to the point of unrecognizability. This effect is attributed to the relatively short wavelength of the commonly used 50-kv. ($\lambda \cong 5 \times 10^{-10}$ cm.) electrons. Although electron diffraction has many advantages over X-ray diffraction in the study of colloidal materials, the foregoing is not one of them. The angle of deviation, 2θ, of a diffracted beam is given by Bragg's law, $2\theta \cong 2 \arcsin \theta = \lambda/d$. The line broadening, B, due to small crystallite size is given by the equation of Laue, $B = 0.9\lambda/t \cos\theta$, where t is the particle size. If θ is less than $\sim 22°$, $\cos\theta$ is approximately constant, and $\arcsin\theta = \theta$. This is the region of θ most generally used for identification. Both B and θ vary directly with λ; thus the resolution is not improved with change in wavelength.

was established for extracting used catalysts: The catalyst was dropped from the reactor (in synthesis gas and at operating temperature) directly into heptane. A representative sample of the catalyst was crushed in a mortar containing heptane, and the wet material was transferred to a small bottle. The bottle was put into a conventional extraction apparatus, and a small funnel was placed in the bottle as shown in figure 33. The condensed toluene flowed into the funnel (which extended to the bottom of the bottle), over the catalyst, and out of the top of the bottle. The catalyst was thus always maintained under liquid toluene to prevent oxidation. To insure removal of the adsorbed hydrocarbons, the samples were extracted for about 72 hours; then the bottle was removed and stoppered.

To make sure that no oxidation occurred during this procedure, a sample of a precipitated catalyst (P3002.1) was reduced in hydrogen at 350° C., transferred to a bottle without contact with air, and stored in heptane. One part of the reduced catalyst was used directly for electron diffraction, and a second sample was extracted with toluene before analysis, as described previously. Both samples produced patterns of metallic iron only.

Figure 34 presents a schematic comparison of the X-ray- and electron-diffraction patterns of metallic iron, magnetite, Hägg carbide, hexagonal close-packed iron carbide, cementite, ϵ-iron nitride, ϵ-iron carbonitride, and magnesium oxide. The data from which these diagrams were prepared are given in table 25. Some of the X-ray patterns were taken from previous work in this laboratory, while others were taken from the tables of Hanawalt, Rinn, and Frevel (*45*). In general, there is good agreement between the X-ray- and electron-diffraction patterns. Complete agreement would not be expected, since there are fundamental differences between electron waves and X-rays. Although the theories of X-ray and electron diffraction are quite similar, Thomson and Cochrane (*82*) have described many practical discrepancies, some of which have been adequately explained.

In the electron-diffraction patterns of the interstitial compounds, iron carbides, nitrides, and carbonitrides, many reflections are missing. On the whole, the electron-diffraction patterns of the other phases are quite complete. Recently, Trillat and Oketani (*83–85*) have published essentially complete electron-diffraction patterns of cementite and Hägg carbide. Their metal specimens were made by evaporating iron on to single crystals of rock salt and then dissolving the salt from the film. Metal prepared in this way is almost entirely strain free, since completely reversible electrodes can

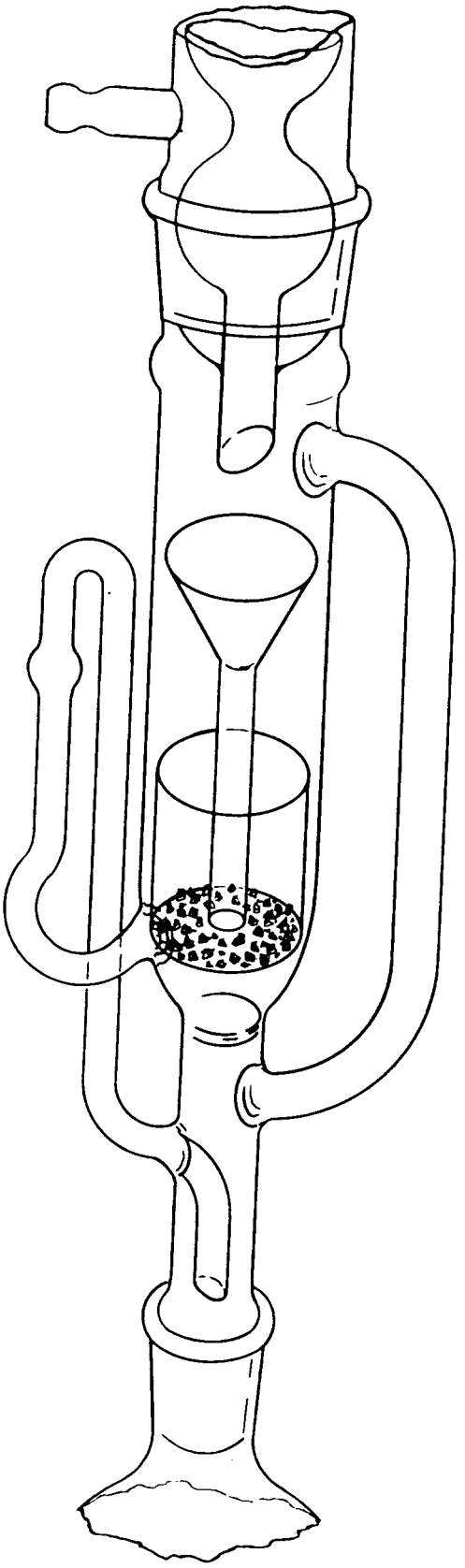

FIGURE 33.—Extraction Apparatus.